A self-pumping lab-on-a-chip for rapid detection of botulinum toxin†

Peter B. Lillehoj,[a] Fang Wei[b] and Chih-Ming Ho*[a]

Received 6th April 2010, Accepted 11th June 2010
DOI: 10.1039/c004885b

A robust poly(dimethylsiloxane) (PDMS) surface treatment was utilized for the development of a self-pumping lab-on-a-chip (LOC) to rapidly detect minute quantities of toxic substances. One such toxin, botulinum neurotoxin (BoNT), is an extremely lethal substance, which has the potential to cause hundreds of thousands of fatalities if as little as a few grams are released into the environment. To prevent such an outcome, a quick (< 45 min) and sensitive detection format is needed. We have developed a self-pumping LOC that can sense down to 1 pg of BoNT type A (in a 1 μL sample) within 15 min in an autonomous manner. The key technologies enabling for such a device are a sensitive electrochemical sensor, an optimized fluidic network and a robust hydrophilic PDMS coating, thereby facilitating autonomous delivery of liquid samples for rapid detection. The stability, simplicity and portability of this device make possible for a storable and distributable system for monitoring bioterrorist attacks.

Introduction

Recent studies modeling the distribution and consumption of milk tainted with BoNT have shown that as little as 10 g released into the supply chain, which is within the capability of terrorists, could cause more than 500,000 causalities in a matter of days.[1] Although current tests, such as mouse bioassay and ELISA, have detection limits well below what is required for this scenario (16 pg/mL and 80 pg/mL respectively), these laboratory-based methods are time consuming (48 and 3 h respectively) making their implementation in the distribution chain impractical.[2,3] Toward the development of a chip-based system, recent work has demonstrated a bead-based sensor which can detect BoNT type A (BoNT/A) toxin within 3.5 h using a fluorescence detection scheme.[4] The next milestone is to develop a fully automated, sub-45 min, portable bio-threat detection system. Microfluidic technologies have the potential to create LOCs that are portable, low-cost and capable of highly sensitive measurements.[5–7] Recent work has led to the development of integrated microsystems for a myriad of applications including DNA analysis,[8,9] polymerase chain reaction,[10–12] optical-based sensing,[13] electrochemical-based sensing,[14] blood separation,[15] immunoassays,[16] and point-of-care diagnostics.[17,18] However, the integration of fluidic components and sensors into a portable, fully functional device that can sense BoNT at lethal concentrations (~100 ng/mL) in under 45 min has yet to be realized.

As the field of microfluidics advances towards a more versatile technology in biology, medicine/healthcare and homeland security, user-friendly LOC systems are required to be uncomplicated, both in fabrication and operation. Previous work has demonstrated the advantages of capillary pumping,[19–23] which offers greater portability, enhanced reliability and simpler operation compared with externally driven systems. Here, we report an autonomous LOC that is able to detect BoNT/A with a sensitivity of 1 ng/mL within 15 min. PDMS is utilized for the fluidic network due to its favorable properties, such as good biocompatibility, optical transparency, ease of fabrication, widespread availability and low cost.[24] A simple, yet highly-stable surface treatment is demonstrated and utilized to produce hydrophilic PDMS microchannels, eliminating the need for externally-powered pumps and greatly simplifying the overall operation. The three-step coating process can be performed in less than 30 min and maintains surface stability for several weeks. Additionally, through optimization of the microfluidic network, only two loading steps are required for the entire detection process allowing for widespread usability. Coupled with a highly sensitive, apatamer-based electrochemical sensor[25,26] and rapid detection system, our device presents an autonomous platform for first response detection of BoNT/A in an unprecedented timely manner.

Experimental

Fabrication materials

Silicon wafers were purchased from Techgophers (Los Angeles, CA) and glass slides were purchased from Fischer Scientific (Tustin, CA). PDMS prepolymer and curing agents (Sylgard 184) were obtained from Dow Corning (Midland, MI) and PEG (MW 200) was obtained from Sigma-Aldrich (St. Louis, MO). Food coloring used for flow visualization was obtained by Tone Brothers (Ankeny, IA). AZ 4620 photoresist (Shipley Corporation), hexamethyldisilazane (HDMS) (Shin-Etsu MicroSi), acetone, isopropanol and methanol (Gallade Chemical), piranha solution and deionized water were provided by the Nanoelectronics Research Facility at the University of California, Los Angeles.

Reagents

HPLC-purified aptamer oligonucleotides, biotin-labeled on the 5′ end and fluorescein-labeled on the 3′ end, were custom-synthesized

[a]*Mechanical and Aerospace Engineering department, University of California, Los Angeles, CA, USA. E-mail: chihming@seas.ucla.edu; Tel: +310-825-9993*
[b]*Dental Research Institute, University of California, Los Angeles, CA, USA*

† Electronic supplementary information (ESI) available: Schematic illustration of the PEG-PDMS coating process, comparison between two fluidic network designs and data showing its effect on BoNT detection sensitivity. See DOI: 10.1039/c004885b

by Operon (Huntsville, AL). Biotin bound to surface streptavidin served as an anchor to the electrode and the fluorescein label allowed for binding of horse radish peroxidase (HRP)-labeled anti-fluorescein antibody to amplify the electrochemical current signal. The 76-bp aptamer nucleotide sequence for BoNT/A detection[27] was: 5′-ATACCAGCTTATTCAATT GAC ATG ACT GGG ATT TTT GGC GAA ATC GAA GGA AGC GGA GAGATAGTAAGTGCAATCT-3′.

Anti-fluorescein antibody was obtained from Roche Applied Science (Indianapolis, IN). BoNT/A toxoid was purchased from Metabiologics (Madison, WI). Polypyrrole (PPy), used for electropolymerization, was obtained from Sigma (St. Louis, MO). 3, 3′, 5, 5′ tetramethylbenzidine substrate (TMB/H_2O_2) was obtained from Neogen (Lexington, KY). Phosphate buffered saline (PBS), 1 × Tris-HCl buffer and ultra pure deionized water (18.3 MΩ·cm) were from Invitrogen (Carlsbad, CA).

Device fabrication

Gold electrodes were fabricated on glass slides and employed as sensors for electrochemical detection. Briefly, glass slides were first exposed to HDMS to enhance adhesion of the photoresist. Photolithography (Karl Suss) was performed to pattern AZ4620 photoresist as a shadow mask for metal evaporation. Chromium and gold were evaporated (CHA Mark 40) onto the glass slides and then lift off was performed through sonication in acetone. PDMS molds were fabricated on silicon wafers, which were first cleaned in a Piranha bath to ensure proper adhesion of photoresist. Photolithography was again performed to pattern AZ 4620 photoresist as an etch mask for subsequent deep reactive ion etching (Unaxis Versaline). Once the molds were fabricated, PDMS prepolymer and curing agents were mixed and degassed. The mixture was poured onto the silicon molds, cured for 2 h at 80 °C, underwent surface modification (see below), cut into individual chips, and inlet and outlet holes were punched. Microfluidic devices for BoNT/A detection were assembled by bonding surface modified PDMS chips with glass slides that were first cleaned in isopropanol and deionized water. Similar to the bonding between untreated PDMS and glass, PEG-coated PDMS and glass exhibit reversible bonding where PDMS chips can be repeatedly removed and re-bonded. Although the bonding is not permanent, no leaking was observed during experimentation.

PDMS surface modification

On-chip BoNT/A detection is facilitated through a quick and robust hydrophilic coating process on PDMS (see Fig. S1 in ESI†) which enables for autonomous transportation of sample fluids. Following curing, PDMS chips were first cleaned in isopropanol and deionized water and dried using compressed air. Chips were exposed to an air plasma using a Harrick air plasma cleaner/sterilizer (Ithaca, NY) for 90 s with the radio frequency set to high. PEG was immediately applied to the oxidized PDMS surface and the chips were placed on a hot plate at 150 °C for 25 min. After heating, the chips were cooled to room temperature and washed with isopropanol and deionized water sequentially to remove residual PEG. Prior to bonding, PDMS chips were thoroughly dried using compressed air.

AFM measurements

Surface topology of untreated PDMS and PEG-coated specimens were captured in air using a Digital Instruments MultiMode Scanning Probe Microscope (SPM) with a Nanoscope 3A controller (Santa Barbara, CA) operating in tapping mode. Specimens were mounted onto steel discs using double-sided adhesive, which were magnetically attached to the stage. Silicon probes (Veeco Probes, Camarillo, CA) were used with a typical tapping frequency of 240–280 kHz and a nominal scanning rate of 0.8–1 Hz. Images were analyzed and processed using Digital Instruments Nanoscope R IIIa software.

Contact angle measurements

To characterize for hydrophilic stability, static contact angle measurements were performed on untreated PDMS, plasma-treated PDMS and PEG-coated PDMS. A First Ten Ångstroms FTÅ4000 contact angle analysis system (Portsmouth, VA) was used to take the measurements. Deionized water droplets of 5 μL were deposited onto the specimens using the system's Nano-Dispense piezo-electric controlled drop dispenser. Six data points were taken on each specimen and analyzed using the system's FTA Video software. All the specimens were stored in polystyrene dishes at room temperature and fresh specimens were used for each measurement.

On-chip BoNT/A detection

Surface modified aptamer-polypyrrole electrodes. The detection electrode consists of conducting PPy polymerized on its thin-film gold surface. For electropolymerization, 10 mM pyrrole diluted in 1 × PBS (pH 7.5) was mixed with 100 nM of BoNT/A biotin/fluorescein-labeled aptamer. A square-wave electrical field was applied for electropolymerization.[28] Each square-wave consisted of 9 s at a potential of +350 mV and 1 s at +950 mV. A total of 30 square-waves cycles was applied and the entire process lasted for 300 s. After polymerization, the electrode was rinsed with ultra pure deionized water and dried under compressed N_2.

Electrochemical detection. The electrochemical sensor is comprised of a working electrode (WE), counter electrode (CE), and a reference electrode (RE). For surface recognition, 1.0 μL of BoNT/A toxoid at varying concentrations, was loaded through inlet 1 of the device and 7 μL of HRP anti-fluorescein antibody in 1 × Tris-HCl buffer (pH = 7.0) was loaded through inlet 2 (inlets 1 and 2 refer to Fig. 3). The loading buffer for the BoNT/A toxoid was a combinational solution of four ions in 1 × Tris-HCl buffer; the concentrations are: NaCl 20 mM, KCl 0.5 mM, $CaCl_2$ 200 mM and $MgCl_2$ 2 mM. The optimization of the combination for the buffer ions was obtained through a closed-loop feedback control experiment. Additionally, it was observed that the addition of detergent in the anti-fluorescein HPR buffer generated bubbles within the fluidic network and thus should be avoided. The two solutions were mixed by passage through the mixing region and driven to the electrode. During the detection process, an electrical field was applied with 20 cycles of 9 s at −300 mV and 1 s at +200 mV. Amperometric measurements were carried out at −200 mV for 60 s following loading of the TMB/H_2O_2 solution through inlet 1. All the sample loading steps were carried out

manually using a pipette and subsequent fluidic processing (liquid transportation, mixing, washing) were carried out autonomously. Baseline measurements (without BoNT loading) were obtained prior to BoNT detection experiments using new chips. The operational protocol for baseline measurements and BoNT detection was identical, with the exception of loading BoNT/A toxoid for the sensing experiments.

Results and discussion

PDMS surface characterization

As a result of the PEG coating, the PDMS channel walls were rendered hydrophilic having a contact angle of $17° \pm 2°$. Atomic force microscopy (AFM) scans of the PEG-coated PDMS revealed uniform hill and valley-shaped features over the surface, representing stacked layers of PEG (Fig. 1). Additionally, the coatings exhibited long-term stability maintaining contact angles $< 22°$ for at least 47 days when stored at room temperature under atmospheric conditions (Fig. 2). Contact angle measurements were limited to this duration due to time constraints; however, the surface coating continues to remain stable, which can be observed from the plot in Fig. 2. Numerous hydrophilic surface coatings on PDMS have been demonstrated such as physical adsorption,[29–32] layer-by-layer assembly,[33–35] electrostatic layer-by-layer self assembly,[36] sol–gel chemistries,[37,38] surface grafting,[39–42] UV grafting,[43] UV-mediated graft polymerization,[44] plasma polymerization,[45] atom-transfer radical polymerization,[46] photo-induced radical polymerization,[47] linking by platinum-catalyzed hydrozilization,[48] and tethering *via* a swelling-deswelling process;[49] our approach involves only three fabrication steps to achieve long-term surface stability and does not dramatically affect the bulk properties of the PDMS. Using this hydrophilic coating, we were able to transport liquids and carry out all the fluidic processes within microchannels by capillary force, thereby obviating the use of external pumps.

Microfluidic design considerations

Utilizing a capillary-based pumping mechanism enables for steady and synchronized flow rates by designing channels with predetermined dimensions. Capillary-driven flows have the advantage of producing steady and preset flow rates, dictated by the channel geometry as shown in the following analysis. The flow rate Q of a capillary-driven system can be expressed by the equation

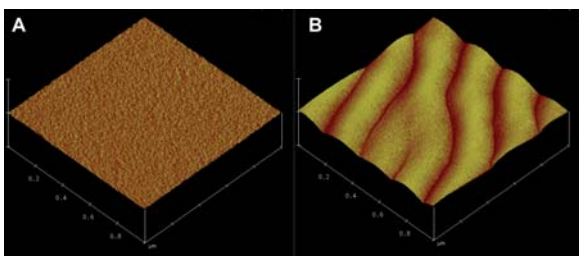

Fig. 1 AFM tapping mode images of (A) untreated PDMS and (B) PEG-coated PDMS. The scan size and z-scale are 1 μm × 1 μm and 100 nm, respectively. Surface-treated PDMS exhibits distinctive hill-like features, representing attached PEG chains, whereas untreated PDMS exhibits a smoother profile.

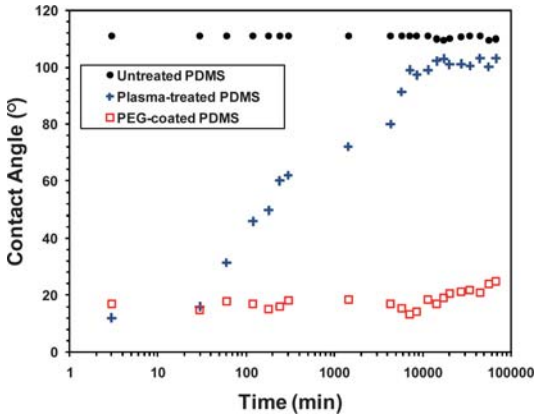

Fig. 2 Long-term stability of PDMS surface modification. A conventional treatment of PDMS by plasma exposure yields relatively short-term surface stability (*i.e.* ~1 h), as opposed to our proposed surface treatment in which a surface stability of ~50 days can be achieved. Untreated PDMS exhibits a contact angle of ~109°.

$Q = 1/\eta\ (\Delta P/R_F)$, where η is the viscosity of the liquid, ΔP is the pressure difference in front of the liquid and R_F is the total flow resistance. Flow resistance in a rectangular channel can be approximated by the equation $R_F = [1/12\ (1 + 5h/6w)\ (hwR^2_H/L)]^{-1}$ when the condition $h < w$ is satisfied, where R_H is the hydraulic radius, L is the length and h, and w are the height and width of the channel, respectively. For such a system, ΔP can be estimated by the capillary pressure Pc at the liquid-air interface in a rectangular microchannel, which can be described by the equation $Pc = -\gamma[(\cos\alpha_t + \cos\alpha_b/h) + (\cos\alpha_l + \cos\alpha_r/w)]$, where γ is the surface tension of the liquid, $\alpha_{t,b,l,r}$ are the contact angles on the top, bottom, left and right walls of the channel, respectively.[50] Based on these equations, it is evident that the flow rates are governed by the geometric dimensions of the channel, since η, γ and α are determined by the liquids being used. Traditionally, individual pumps are required for each inlet, but this greatly increases the complexity and bulkiness of a bio-detection system. Furthermore, precise coordination of flow rates using multiple pumps is extremely challenging and usually requires additional control components. We are able to produce steady and synchronized flow rates by designing the channels with identical dimensions. With such controllability, microfluidic networks can be designed for specific applications which require precise flow rates or timed fluidic processes and reactions.

Device design and optimization

The proposed device (Fig. 3) is comprised of two independent inlet reservoirs and one outlet reservoir having diameters 2 mm and 1 mm respectively. The inlet reservoirs are specifically designed for the sample and reporter solutions, which can be loaded independently *via* a pipette or simultaneously for improved automation. The inlet and mixing channels are 200 μm wide whereas both serpentine channels are 400 μm wide. All microchannels are 115 μm in height. A 2 mm circular chamber is situated between the inlet and the mixing channel to provide a region for the sample and reporter solutions to merge and mix. Further downstream is a mixing region, consisting of a zigzag-shaped channel, which flows into a closely-packed serpentine

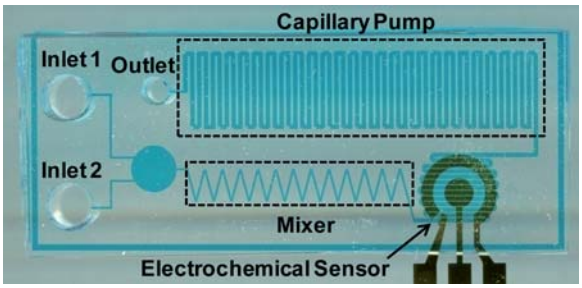

Fig. 3 A photograph of the integrated lab-on-a-chip for rapid BoNT/A detection. The device is filled with dye for enhanced visualization of the microfluidic network.

channel situated over the electrode. The second rectangular serpentine channel functions as a capillary pump to pull liquids through the fluidic network. Specifically, this channel enables the TMB/H_2O_2 substrate to completely wash and flush the sample and reporter solutions from the electrode surface. Sample loading was achieved by introducing liquids into the inlet reservoirs of the device. Liquids quickly filled the channels upon contact due to their hydrophilic nature such that a 15 μL sample could be loaded in less than 1 min. Lastly, the liquid column locations within the channels were precisely controlled through carefully regulation of liquid volumes (*via* a pipette).

Several iterations for improving the microchannel network were performed where each iteration incorporated several design changes to enhance device functionality. Two final designs (Fig. S2 in ESI†) were chosen for further optimization to enhance the detection sensitivity. From our observations, encasing the electrode in an enclosed chamber, as shown in Fig. S2B, generated non-uniform fluid flow and resulted in inadequate surface coverage of the electrode. In contrast, designing a closely-packed serpentine channel over the electrode, as shown in Fig. S2A, improved surface coverage and provided higher signals readings during detection. Additionally, by increasing the width of the rectangular serpentine channel from 200 μm to 400 μm, a larger volume of TMB/H_20_2 solution could flow through the fluidic network. This allowed for improved washing of the sample and reporter solutions from the electrode surface, which resulted in higher detection sensitivity (Fig S3 in ESI†).

BoNT/A detection

BoNT detection is achieved by combining an electrochemical method with enzymatic amplification using an aptamer probe with a target-induced conformational change to detect BoNT/A toxoid.[51,52] All experiments were performed using the nontoxic purified BoNT/A light chain. The aptamer is dually-labeled with reporting (fluorescein) and anchoring (biotin) tags. In the absence of BoNT/A, the aptamer remains in the closed state and steric hindrance from the sensor surface inhibits the anti-fluorescein antibody from accessing the reporting tag (Fig. 4A). In the presence of BoNT/A, the aptamer changes its conformation, enabling the antibody to bind to the reporter, thus, generating an electrochemical current signal through its HRP moiety (Fig. 4B). Therefore, only the specific BoNT/A target can generate an amplified current.

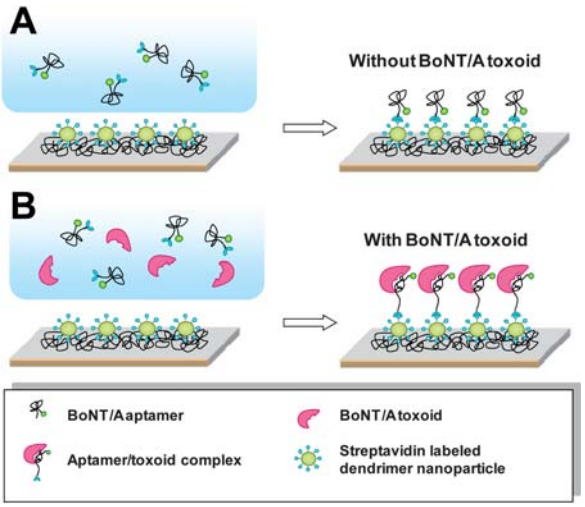

Fig. 4 A schematic illustration of the BoNT/A detection scheme. (A) In the absence of BoNT/A, the aptamer remains in a closed state and steric hindrance from the sensor surface inhibits signal amplification. (B) In the presence of BoNT/A toxoid, it binds to the aptamer thus altering its conformation and exposing the fluorescein tag for reaction with HRP-labeled anti-fluorescein antibody allowing for an electrochemical current to be generated.

For validation of BoNT/A specificity, different targets were studied (Fig. 5A). The detection signals generated by irrelevant proteins approximated those of the blank control in the absence of a sample addition. Only the BoNT/A sample resulted in a high signal readout (signal-to-background ratio (SBR) = 5.6 at 100 ng/mL). Such high specificity can be attributed to the correct folding and recognition of the aptamer for BoNT/A toxoid. To further prove the sensitivity of our device, experiments were performed at different concentrations of BoNT/A target toxoid (Fig. 5B). In this calibration curve, an optimized ion buffer with four ions is utilized to improve the signal-to-noise ratio (SNR). From concentrations of 1000 ng/mL to 0.8 ng/mL, our system exhibits a good dynamic response where the cutoff between the blank control and the sample is around 1 ng/mL. The detection current at these concentration of BoNT/A is approximately 1000–60 nA, which allows for the usage of commercial hand-held current readers, thus maintaining portability.[53]

In addition to utilizing BoNT aptamers and steric-enhanced-signal amplification, the sensitivity of BoNT/A detection is highly dependent on sample loading and washing processes, which are dictated by the design of the fluidic network. BoNT detection was performed on two distinctly-designed chips (Fig. S2) to compare their effects on the detection sensitivity. Based on the plot in Fig. S3, we see that optimization of the fluidic network has a notable impact on the output signal; design 1 produced a SBR of 5.6, whereas design 2 produced a SBR of 1.6. For such high sensitivity measurements in which very small concentrations of BoNT are being detected, the noise levels are highly prone to fluctuations which arise from various experimental factors, including non-specific binding, electrode surface irregularities and non-uniform probe immobilization and polypyrrole coatings. Therefore, optimization of the fluidic network was crucial for enhancing the output signal and detection sensitivity.

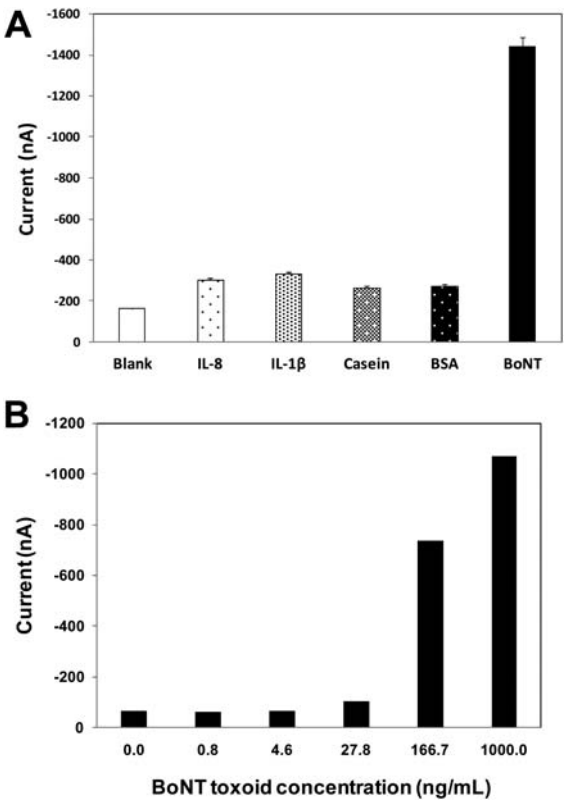

Fig. 5 (A) Comparison between BoNT/A and irrelevant proteins, demonstrating the detection specificity of the sensor against BoNT. Experiments were performed in open air with manual sample loading. (B) System response of varying BoNT/A concentrations. The entire detection process was achieved "on-chip" within 15 min.

In addition to obtaining high-sensitivity measurements, the autonomous nature of this system enables for simplified operation, which is crucial for widespread usage and on-site monitoring. The detection of real samples would follow closely to the experimental protocol presented in this work. Briefly, the sample of interest and an HRP anti-fluorescein antibody solution would be loaded into inlets 1 and 2 of the device. A pulsed electric field would be applied to the electrode, followed by the loading of a TMB/H_2O_2 solution and subsequent amperometric measurements. Ultimately, these results demonstrate the ability to perform fast and simple detection of BoNT/A with a sensitivity of 1 pg (1 μL sample), where the entire detection scheme can be achieved within 15 min.

Conclusions

By developing a simple and robust hydrophilic coating technique on PDMS, we have fabricated a fully-functional lab-on-a-chip for the detection of potential bioterror agents using BoNT/A as a model system. Our device detected 1 ng/mL of BoNT/A in less than 15 min, well below the specifications for the identification of large-scale bioterror attacks using BoNT.[1] Further optimization of the detection protocol and the channel geometry for faster flow rates will allow for higher detection sensitivity and shorter detection time. Furthermore, changing the aptamer specificity will allow for the detection of other analytes that are relevant to everyday applications, such as medical diagnosis, environmental and food safety monitoring and diagnostic systems for the developing world.

Acknowledgements

This work was generously funded by the following agencies: NIH Pacific Southwest Center (UC Irvine/NIH 2005-1609 : 03) (UO1DE017790), NSF SINAM Center (DMI-0327077), NIH CCC Center (NIH/Nat'l Eye Inst. 5 PN2EY018228:02), OFNASET (NIDCR UO3 DE-06-003) and the UCLA Graduate Research Mentorship Fellowship. The authors thank Vye-Chi Low for assisting with the AFM scans and Dr Robin Garrell's laboratory for use of their contact angle analysis system. We also thank Dr T. S. Wong and Dr E. Lillehoj for their useful comments in reviewing the manuscript.

References

1 L. M. Wein and Y. Liu, *Proc. Natl. Acad. Sci. U. S. A.*, 2005, **102**, 9984–9989.
2 E. J. Schantz and J. Sugiyama, *J. Agric. Food Chem.*, 1974, **22**, 26–30.
3 J. L. Ferreira, S. Maslanka, E. Johnson and M. Goodnough, *J. AOAC Int.*, 2003, **86**, 314–331.
4 M. L. Frisk, E. Berthier, W. H. Tepp, E. A. Johnson and D. J. Beebe, *Lab Chip*, 2008, **8**, 1793–1800.
5 C. M. Ho and Y. C. Tai, *Annu. Rev. Fluid Mech.*, 1998, **30**, 579–612.
6 D. C. Duffy, J. C. McDonald, O. J. A. Schueller and G. M. Whitesides, *Anal. Chem.*, 1998, **70**, 4974–4984.
7 M. A. Unger, H. Chou, T. Thorsen, A. Scherer and S. R. Quake, *Science*, 2000, **288**, 113–116.
8 R. Pal, M. Yang, R. Lin, B. N. Johnson, N. Srivastava, S. Z. Razzacki, K. J. Chomistek, D. C. Heldsinger, R. M. Haque, V. M. Ugaz, P. K. Thwar, Z. Chen, K. Alfano, M. B. Yim, M. Krishnan, A. O. Fuller, R. G. Larson, D. T. Burked and M. A. Burns, *Lab Chip*, 2005, **5**, 1024–1032.
9 M. A. Burns, B. N. Johnson, S. N. Brahmasandra, K. Handique, J. R. Webster, M. Krishnan, T. S. Sammarco, P. M. Man, D. Jones, D. Heldsinger, C. H. Mastrangelo and D. T. Burke, *Science*, 1998, **282**, 484–487.
10 N. Ramalingam, H.-B. Liu, C.-C. Dai, Y. Jiang, H. Wang, Q. Wang, K. M. Hui and H.-Q. Gong, *Biomed. Microdevices*, 2009, 1572–8781.
11 R. H. Liu, J. Yang, R. Lenigk, J. Bonanno and P. Grodzinski, *Anal. Chem.*, 2004, **76**, 1824–1831.
12 C.-Y. Lee, G.-B. Lee, J.-L. Lin, F.-C. Huang and C.-S. Liao, *J. Micromech. Microeng.*, 2005, **15**, 1215–1223.
13 S. Balslev, A. M. Jorgensen, B. Bilenberg, K. B. Mogensen, D. Snakenborg, O. Geschke, J. P. Kutter and A. Kristensen, *Lab Chip*, 2006, **6**, 213–217.
14 Z. Zou, J. Hana, A. Jang, P. L. Bishop and C. H. Ahn, *Biosens. Bioelectron.*, 2007, **22**, 1902–1907.
15 S. Thorslund, O. Klett, F. Nikolajeff, K. Markides and J. Bergquist, *Biomed. Microdevices*, 2006, **8**, 73–79.
16 S. K. Sia, V. Linder, B. A. Parviz, A. Siegel and G. M. Whitesides, *Angew. Chem., Int. Ed.*, 2004, **43**, 498–502.
17 V. Srinivasan, V. K. Pamula and R. B. Fair, *Lab Chip*, 2004, **4**, 310–315.
18 C. H. Ahn, J.-W. Choi, G. Beaucage, J. H. Nevin, J.-B. Lee, A. Puntambekar and J. Y. Lee, *Proc. IEEE*, 2004, **92**, 154–173.
19 D. Juncker, H. Schmid, U. Drechsler, H. Wolf, M. Wolf, B. Michel, N. de Rooij and E. Delamarche, *Anal. Chem.*, 2002, **74**, 6139–6144.
20 T. Vestad, D. W. M. Marr and J. Oakey, *J. Micromech. Microeng.*, 2004, **14**, 1503–1506.
21 M. Zimmermann, H. Schmid, P. Hunzikerb and E. Delamarche, *Lab Chip*, 2007, **7**, 119–125.
22 R. Lovchik, C. von Arx, A. Viviani and E. Delamarche, *Anal. Bioanal. Chem.*, 2008, **390**, 801–808.
23 M. Zimmermann, P. Hunziker and E. Delamarche, *Biomed. Microdevices*, 2009, **11**, 1–8.
24 D. C. Duffy, J. C. McDonald, O. J. A. Schueller and G. M. Whitesides, *Anal. Chem.*, 1998, **70**, 4974–4984.

25 T. J. Huang, M. Liu, L. D. Knight, W. W. Grody, J. F. Miller and C. M. Ho, *Nucleic Acids Res.*, 2002, **30**, 55e.
26 S. Cai, B. R. Singh and S. Sharma, *Crit. Rev. Microbiol.*, 2007, **33**, 109–125.
27 J. B. H. Tok and N. O. Fischer, *Chem. Commun.*, 2008, 1883–1885.
28 F. Wei and C. M. Ho, *Anal. Bioanal. Chem.*, 2009, **393**, 1943–1948.
29 S. Thorslund, R. Larsson, F. Nikolajeff, J. Bergquist and J. Sanchez, *Sens. Actuators, B*, 2007, **123**, 847–855.
30 D. S. Bodas and C. Khan-Malek, *Sens. Actuators, B*, 2007, **120**, 719–723.
31 D. Wu, Y. Luo, X. Zhou, Z. Dai and B. Lin, *Electrophoresis*, 2005, **26**, 211–218.
32 S. Lee and J. Vörös, *Langmuir*, 2005, **21**, 11957–11962.
33 Y. Xiao, X. D. Yu, J. J. Xu and H. Y. Chen, *Electrophoresis*, 2007, **28**, 3302–3307.
34 A. J. Wang, J. J. Xu and H. Y. Chen, *J. Chromatogr., A*, 2006, **1107**, 257–264.
35 W. Wang, L. Zhao, J. R. Zhang, X. Wang, J. J. Zhu and H. Y. Chen, *J. Chromatogr., A*, 2006, **1136**, 111–117.
36 H. Makamba, Y. Y. Hsieh, W. C. Sung and S. H. Chen, *Anal. Chem.*, 2005, **77**, 3971–3978.
37 G. T. Roman, T. Hlaus, K. J. Bass, T. G. Seelhammer and C. T. Culbertson, *Anal. Chem.*, 2005, **77**, 1414–1422.
38 G. T. Roman and C. T. Culberston, *Langmuir*, 2006, **22**, 4445–4451.
39 D. Wu, J. Qin and B. Lin, *Lab Chip*, 2007, **7**, 1490–1496.
40 J. M. Wu, Y. Chung, K. J. Belford, G. D. Smith, S. Takayama and J. Lahann, *Biomed. Microdevices*, 2006, **8**, 99–107.
41 G. Sui, J. Wang, C. C. Lee, W. Lu, S. P. Lee, J. V. Leyton, A. M. Wu and H. R. Tseng, *Anal. Chem.*, 2006, **78**, 5543–5551.
42 E. Delamarche, C. Donzel, F. S. Kamounah, H. Wolf, M. Geissler, R. Stutz, P. Schmidt-Winkel, B. Michel, H. J. Mathieu and K. Schaumburg, *Langmuir*, 2003, **19**, 8749–8758.
43 S. Hu, X. Ren, M. Bachman, C. E. Sims, G. P. Li and N. Allbritton, *Langmuir*, 2004, **20**, 5569–5574.
44 S. Hu, X. Ren, M. Bachman, C. E. Sims, G. P. Li and N. Allbritton, *Anal. Chem.*, 2004, **76**, 1865.
45 V. Barbier, M. Tatoulian, H. Li, F. Arefi-Khonsari, A. Ajdari and P. Tabeling, *Langmuir*, 2006, **22**, 5230–5232.
46 D. Xiao, T. V. Le and M. J. Wirth, *Anal. Chem.*, 2004, **76**, 2055–2061.
47 T. Goda, T. Konno, M. Takai, T. Moro and K. Ishihara, *Biomaterials*, 2006, **27**, 5151–5160.
48 H. Chen, Z. Zhang, Y. Chen, M. A. Brook and H. Sheardown, *Biomaterials*, 2005, **26**, 2391–2399.
49 K. Yu and Y. Han, *Soft Matter*, 2006, **2**, 705–709.
50 J. H. Spurk, *Strömungslehre*, 2004, Springer, Berlin, 164.
51 F. Wei and C. M. Ho, *Nucleic Acids Res.*, 2008, **36**, e65.
52 S. P. Song, L. H. Wang, J. Li, J. L. Zhao and C. H. Fan, *TrAC, Trends Anal. Chem.*, 2008, **27**, 108–117.
53 S. Joo and R. B. Brown, *Chem. Rev.*, 2008, **108**, 638–651.